Amperometric biosensors based on carboxylated multiwalled carbon nanotubes-metal oxide nanoparticles-7,7,8,8-tetracyanoquinodimethane composite for the determination of xanthine

Berna Dalkıran, Pınar Esra Erden, Esma Kılıç

www.elsevier.com/locate/talanta

PII: S0039-9140(17)30222-9
DOI: http://dx.doi.org/10.1016/j.talanta.2017.02.021
Reference: TAL17297

To appear in: *Talanta*

Received date: 18 November 2016
Revised date: 3 February 2017
Accepted date: 7 February 2017

Cite this article as: Berna Dalkıran, Pınar Esra Erden and Esma Kılıç Amperometric biosensors based on carboxylated multiwalled carbon nanotubes metal oxide nanoparticles-7,7,8,8-tetracyanoquinodimethane composite for th determination of xanthine, *Talanta* http://dx.doi.org/10.1016/j.talanta.2017.02.021

Amperometric biosensors based on carboxylated multiwalled carbon nanotubes-metal oxide nanoparticles-7,7,8,8-tetracyanoquinodimethane composite for the determination of xanthine

Berna Dalkıran, Pınar Esra Erden*, Esma Kılıç

Ankara University, Faculty of Science, Department of Chemistry, Ankara, Turkey

*Corresponding author. Tel.: +903122126720/1278; Fax.: +903122232395.
erdenpe@gmail.com

Abstract

A comparison of the analytical performances of two xanthine biosensors, based on the use of different metal oxide nanoparticles (MONPs: Co_3O_4 or Fe_3O_4)-modified carboxylated multiwalled carbon nanotubes (c-MWCNTs)-7,7′,8,8′-tetracyanoquinodimethane (TCNQ)-chitosan (CHIT) composite, is discussed. Xanthine oxidase (XOD) enzyme was covalently attached to c-MWCNTs/MONPs/TCNQ/CHIT/GCE via N-ethyl-N'-(3-dimethylaminopropyl) carbodiimide (EDC) and N-hydroxy succinimide (NHS) chemistry and the electrode surface was further modified with Nafion in order to minimize the effect of possible interfering substances. The results showed that analytical performance of the Fe_3O_4 based biosensor was better than the Co_3O_4 based biosensor. The linear working range range, limit of detection and sensitivity were found to be 1.9×10^{-6} – 2.3×10^{-4} M, 0.20 μM (*S/N*=3), 25.07 $\mu AmM^{-1}cm^{-2}$ for the Fe_3O_4 based biosensor and 1.9×10^{-6}–1.2×10^{-4} M, 0.36 μM (*S/N*=3), 13.24 $\mu AmM^{-1}cm^{-2}$ for the Co_3O_4 based biosensor, respectively. The purposed biosensors were applied in the determination of xanthine in coffee samples, and satisfactory results were obtained.

Graphical Abstract

Keywords: Xanthine biosensor; Co_3O_4 nanoparticles; Fe_3O_4 nanoparticles; Mediator; Multiwalled carbon nanotubes

1. Introduction

Electrochemical biosensors combine the sensitivity of electroanalytical methods with the bioselectivity of the biological component [1]. These devices have found promising applications in various fields such as biotechnology, food industry, health care, medicine and enviromental monitoring due to their favourable characteristics like high sensitivity, specificity, speed, portability, independence of sample turbidity and low cost [2, 3]. Carbon nanotubes (CNTs) represents an important group of nanomaterials which have attracted a huge attention in biosensor construction due to their unique electronic, metallic, and structural characteristics. They have large surface area, good mechanical strength, high electrical conductivity, fine biocompatibility, functional surface and good chemical stability [4]. Carbon nanotubes based biosensors have been found to be superior to traditional carbon electrode based biosensors in terms of detection limit, sensitivity and selectivity [3].

The use of metal oxide nanoparticles in the fabrication of biosensors is also of great interest as they exhibit unique physical, chemical and catalytic properties [5]. It is well known that metal oxide nanoparticles not only have high surface area, good biocompatibility, strong adsorption ability and chemical stability, but also display rapid electron transfer kinetics [6]. Fe_3O_4-NPs have been widely used in biosensing applications because of their favorable characteristics i.e., strong superparamagnetic property, high electron communication and low toxicity [7]. On the other hand, another popular metal oxide, Co_3O_4-NPs continue to attract significant interest due to their wide availability, high chemical stability and excellent electrocatalytic activity [8, 9].

MWCNTs and MONPs have been proven to be good a material combination for preparing high performance nanocomposites [10]. Previous studies have shown that MWCNTs and MONPs nanocomposite resulted in large electrochemical surface area and fast electron

transfer for biosensor applications [11, 12]. Up to now, various MONPs-CNTs composites such as Fe_3O_4–MWCNTs [13], ZnO–MWCNTs [14], Co_3O_4–MWCNTs [8], TiO_2–MWCNTs [15], NiO–MWCNTs [16], Bi_2O_3–MWCNTs [11], Fe_3O_4–c-MWCNTs [17] have been used in biosensor construction. These nanocomposites have been reported to improve the analytical characteristics of the biosensors.

Xanthine (3,7-dihydro-1H-purine-2,6-dione) is a purine base generated from guanine by guanine deaminase and from hypoxanthine by xanthine oxidase [18]. Xanthine concentration in human body fluids is used as a marker of pathological conditions such as xanthinuria, renal insufficiency or gout [19]. Coffee is a soft beverage widely and frequently consumed in the world. The xanthine alkoloids including caffeine, theophylline and theobromine are present in coffee, tea and cocoa and known as mild stimulants [20]. Moreover, the monitoring of xanthine concentration can be used as an index for estimating the degree of meat freshness or spoilage [21]. Therefore, development of fast and reliable methods for xanthine determination is of great significance in clinical diagnostics and food industry. Different methods have been reported to determine xanthine e.g. gas chromatography [22], capillary electrophoresis [23], HPLC [24, 25] and spectrophotometry [26]. Common drawbacks of these techniques are the cumbersome procedure for sample preparation, requiring expert handling and costly equipment. Nowadays electrochemical biosensors, have become a encouraging alternative of the conventional analytical methods because a low detection limit, good selectivity, high sensitivity and real time monitoring can be achieved with this technique. Many amperometric biosensors for xanthine determination have been developed [8, 27-29]. These biosensors are generally based on the determination of enzymatically generated H_2O_2 and/or uric acid [28, 30] or consumption of O_2 during the enzymatic reaction [31]. Artificial mediators (second generation type) are widely used in biosensor construction in order to improve the selectivity and sensitivity of amperometric biosensing. The function of artificial mediator is to shuttle electrons between the active site of the enzyme and the electrode to allow detection at low potentials. This strategy can minimize interference with coexisting electroactive species [32]. Various mediators including ferrocene or its derivatives [19, 33] 1,4-benzoquinone [19] Prussian Blue [34] and cobalt phthalocyanine-ferricyanide [35] have been utilized for the

fabrication of xanthine biosensors. TCNQ has being used as mediator in the fabrication of biosensors, because it has great number of properties, as high electric conductivity [36].

This study describes, for the first time, the use of the combination of MONPs (Co_3O_4 or Fe_3O_4), c-MWCNTs and TCNQ in a matrix of CHIT to develop new xanthine biosensors. Analytical performances of the Co_3O_4 and Fe_3O_4 based biosensors in terms of detection limit, sensitivity, selectivity, repeatability, and long term stability were compared. Furthermore, the applicability of the biosensors for the analysis of xanthine in coffee was investigated.

2. Experimental

2.1. Reagents and Solutions

XOD (E.C. 1.17.3.2 from Microbial source with a specific activity of ≥7 Units/mg solid), Co_3O_4 nanoparticles (<50 nm particle size (TEM), 99.5% trace metals basis), Fe_3O_4 nanoparticles (50-100 nm particle size (TEM), 97% trace metals basis), $K_3Fe(CN)_6$, $K_4Fe(CN)_6.3H_2O$, uric acid, ascorbic acid, sodium dihydrogen phosphate dihydrate and disodium hydrogen phosphate dihydrate, EDC, NHS and Nafion (perfluorinated resin solution, 5 wt% in lower aliphatic alcohol and water mixture) were purchased from Sigma (St. Louis, MO, USA). Xanthine and glucose were purchased from Fluka (Buchs, Switzerland). c-MWCNTs (O.D.<8 nm; I.D. 2-5nm; length 10–30 μm) were bought from Cheaptubes Inc. (Brattleboro, USA). Chitosan (90% deacetylation, medium molecular weight) and 7,7,8,8-tetracyanoquinodimethane were obtained from Aldrich. Standard xanthine solutions were prepared by dissolving xanthine in 0.10 M NaOH. All aqueous solutions were prepared using double distilled water.

2.2. Apparatus and Measurements

A computerized IVIUM electrochemical analyzer (Ivium Technologies, Netherlands) was used for the electrochemical measurements. A glassy carbon electrode (3 mm in diameter), a platinum wire (BAS MW 1034) and Ag/AgCl electrode (BAS MF 2052) were used as working, auxiliary and reference electrodes, respectively. Scanning electron microscopy (SEM) was performed using Carl Zeiss AG, EVO® 50 Series. Cyclic voltammetry (CV) and electrochemical impedance spectroscopy (EIS) measurements were recorded in a solution of 5.0 mM $K_3[(Fe(CN)_6]$, 5.0 mM $K_4[(Fe(CN)_6]$ with 0.5 M KCl. CVs were recorded between (–1.0)V – (+1.0)V at a scan rate of 50 mV s^{-1}. Impedance experiments were performed at 0.2 V with a frequency range of 10^6 Hz-0.5 Hz and plotted in the form of complex plane diagrams (Nyquist plots). HPLC measurements were conducted on a system consisting of a Shimadzu LC-20AT pump, a Shimadzu SPD-20A UV detector and a Inertsil ODS-3 (250 × 4.6 mm, 5 µm) column, Shimadzu CTO-20A oven. The supporting electrolyte used for the electrochemical studies was 0.05 M pH 7.0 phosphate buffer solution (PBS). The test solution was deoxygenated with high purity N_2 gas for 15 min before each experiment, and N_2 blanket was kept over the solution to maintain an inert atmosphere during the measurements. All measurements were performed at room temperature.

2.3. Biosensor Preparation

GCE surface was polished with 0.05 µm alumina powder and was consecutively sonicated with ethanol and double distilled water for 5 min. CHIT solution was prepared by adding 0.025 g of CHIT flakes in 5.0 mL of acetate buffer solution (pH 5.0) and stirring at room temperature until complete dissolution was achieved. The c-MWCNTs, Co_3O_4-NPs and TCNQ were ultrasonicated in CHIT solution for 4 h to give a final concentration of 1 mg mL^{-1} c-MWCNTs, 0.5 mg mL^{-1} Co_3O_4-NPs and 9 mg mL^{-1} TCNQ, respectively. For comparison, Fe_3O_4-NPs modified biosensor was also prepared with the same method: c-MWCNTs, Fe_3O_4-NPs and TCNQ were sonicated for 4 h, until a homogenous dispersion containing 1 mg mL^{-1} c-MWCNTs, 1 mg mL^{-1} Fe_3O_4-NPs and 6 mg mL^{-1} TCNQ was obtained. c-MWCNTs/MONPs/TCNQ/CHIT suspension showed good stability for up to one

month. Therefore, the c-MWCNTs/MONPs/TCNQ/CHIT suspension was prepared once a month. This suspension was sonicated for 10 min before every use. In both cases, 10 µL of the c-MWCNTs/MONPs/TCNQ/CHIT suspension was casted onto the surface of the pre-cleaned GCE and allowed to dry slowly. XOD solution (0.025 Units μL^{-1}) prepared in 0.05 M pH 7.0 PBS was immobilized onto c-MWCNTs/MONPs/TCNQ/CHIT/GCE using EDC−NHS coupling chemistry. 5 µL of 50 mM EDC–200 mM NHS solution (in 0.05 M pH 7.0 PBS) was dropped on the c-MWCNTs/MONPs/TCNQ/CHIT modified electrode surface and dried in air. 10 µL of XOD was casted onto the electrode surface and left to dry. Finally, 7.5 µL (0.25%) of Nafion was casted on the enzyme electrode and dried. The biosensor was then washed in PBS (pH 7.0) to remove all the unbound components. The prepared biosensors were stored in a refrigerator, when not in use. The biosensor fabrication procedure is shown in Scheme 1.

Scheme 1. The fabrication procedure for the XOD/c-MWCNTs/MONPs/TCNQ/CHIT/GCE.

3. Results and discussion

3.1. Surface morphological characterization studies using SEM

The surface morphologies of CHIT, c-MWCNTs/CHIT, c-MWCNTs/Co_3O_4/CHIT, c-MWCNTs/Fe_3O_4/CHIT, c-MWCNT/Co_3O_4/TCNQ/CHIT, c-MWCNT/Fe_3O_4/TCNQ/CHIT and XOD/c-MWCNTs/Co_3O_4/TCNQ/CHIT modified GCEs were studied by SEM as shown in Figure 1. The SEM image of CHIT modified GCE (image a) shows a featureless morphology. Image b shows that the c-MWCNTs were uniformly dispersed in chitosan matrix. Image c and d shows that the MONPs were also dispersed in the c-MWCNTs/CHIT matrix without obvious aggregation. The porous structure of the c-MWCNTs/MONPs/CHIT composite can increase the effective surface area of the electrode and thus facilitate the diffusion of xanthine into the composite. On the other hand, image e and f shows well defined different structures indicating that TCNQ molecules were incorporated into the c-

MWCNT/MONPs/CHIT matrix. The large surface area of MWCNT and MONPs and porous nature of the c-MWCNT/MONPs/TCNQ/CHIT composite offers a good platform for immobilizing XOD molecules. After the immobilization of XOD onto c-MWCNTs/Co_3O_4/TCNQ/CHIT/GCE, the porous morphology changed to a regular form with bright structures (image g). This indicates that XOD was immobilized onto the c-MWCNTs/MONPs/TCNQ/CHIT/GCE.

Fig. 1. SEM images of (a) CHIT/GCE, (b) c-MWCNTs/CHIT/GCE,
(c) c-MWCNT/Co_3O_4/CHIT/GCE, (d) c-MWCNT/Fe_3O_4/CHIT/GCE,
(e) c-MWCNT/Co_3O_4/TCNQ/CHIT/GCE (f) c-MWCNT/Fe_3O_4/TCNQ/CHIT/GCE
(g) XOD/c-MWCNT/Co_3O_4/TCNQ/CHIT/GCE.

3.2. Electrochemical behaviour of modified electrodes

CV was performed using the redox couple $[Fe(CN)_6]^{3-}$/$[Fe(CN)_6]^{4-}$ in order to investigate the electrochemical behavior of different modified GCEs and the results are depicted in Fig. 2. Well-defined redox peaks were observed at the bare GCE (curve b). The modification of GCE by CHIT film resulted in a marked decrease in the peak current signal (curve a). This decrease can be attributed to the barrier effect of the CHIT film towards the redox probe. This effect leads to a decrease of the $[Fe(CN)_6]^{3-/4-}$ current signal. Meanwhile, an increase in the peak potential separation (ΔEp) due to a decrease of the electrochemical reversibility of the redox couple at the CHIT/GCE was observed. In contrast, with MONPs/CHIT/GCE a remarkable current increase and ΔEp decrease were observed (curves c and d). This indicates that the MONPs/CHIT composite exhibited better conductivity than the CHIT film and facilitated the electron transfer. When c-MWCNTs were introduced into CHIT matrix, the peak separation decreased and both the anodic and cathodic peak currents (I_p) increased significantly. suggesting enhanced electron transfer, facilitated by the large surface area provided by the c-MWCNTs (curve e). For the c-MWCNTs/Co_3O_4/CHIT/GCE (curve f) (ΔEp:125 mV, i_{pa}:175 μA), and c-MWCNTs/Fe_3O_4/CHIT/GCE (curve g) (ΔEp:150 mV, i_{pa}:200 μA) the peak

currents increased more and ΔEp became smaller compared with the CHIT/GCE (ΔEp:500 mV, i_{pa}:35 μA) or MONPs/CHIT (Co_3O_4/CHIT/GCE; ΔEp:275 mV, i_{pa}:95 μA) modified electrodes. Moreover, the highest current response was obtained with the c-MWCNTs/Fe_3O_4/CHIT/GCE. The possible reason for this enhanced response is the large surface area and high conductivity of c-MWCNTs–MONPs composite offered by the synergistic effect of two highly conducting materials MONPs and c-MWCNTs. The synergistic effects can be attributed to the excellent electron transfer ability of c-MWCNTs and MONPs.

The electroactive surface area of the modified electrodes was estimated with CV according to the Randles–Sevick equation [37] that is, $i_p=2.69\times10^{-5}AD^{1/2}n^{3/2}v^{1/2}C$. In this equation n is the number of electrons transferred (n=1), A refers to the effective surface area of the electrode (cm^2), D is the diffusion coefficient for $[Fe(CN)_6]^{3-}$ (7.6×10^{-6} cm^2s^{-1}), v refers to the scan rate ($V\ s^{-1}$) and C is the concentration of $[Fe(CN)_6]^{3-}$. By applying the Randles–Sevcik equation the calculated effective surface area was 0.071 cm^2, 0.055 cm^2, 0.109 cm^2, 0.125 cm^2, 0.190 cm^2, 0.210 cm^2 and 0.240 cm^2 for GCE, CHIT/GCE, Co_3O_4/CHIT/GCE, Fe_3O_4/CHIT/GCE, c-MWCNTs/CHIT/GCE, c-MWCNTs/Co_3O_4/CHIT/GCE and c-MWCNTs/Fe_3O_4/CHIT/GCE, respectively. In comparison with the bare GCE, the effective surface areas of the Co_3O_4/CHIT/GCE, Fe_3O_4/CHIT/GCE, c-MWCNTs/CHIT/GCE, c-MWCNTs/Co_3O_4/CHIT/GCE and c-MWCNTs/Fe_3O_4/CHIT/GCE were increased by about 1.5, 1.8, 2.8, 3.0 and 3.4 times, respectively. The results show that c-MWCNTs/Fe_3O_4/CHIT/GCE can provide facile electron transfer and more binding sites for electroactive substance than other modified electrodes.

Fig. 2. (A) Cyclic voltammograms of (a) CHIT/GCE, (b) GCE, (c) Co_3O_4/CHIT/GCE, (d) Fe_3O_4/CHIT/GCE, (e) c-MWCNTs/CHIT/GCE, (f) c-MWCNTs/Co_3O_4/CHIT/GCE, and (g) c-MWCNTs/Fe_3O_4/CHIT/GCE at 50 mVs^{-1} (B) The Nyquist curves of in (a) CHIT/GCE, (b) GCE, (c) Co_3O_4/CHIT/GCE, (d) Fe_3O_4/CHIT/GCE, (e) c-MWCNTs/CHIT/GCE, (f) c-MWCNTs/Co_3O_4/CHIT/GCE, and (g) c-MWCNTs/Fe_3O_4/CHIT/GCE 0.50 M KCl solution containing 5.0 mM $Fe(CN)_6^{3-/4-}$

Impedance spectroscopy is an effective tool for probing the features of a surface-modified electrodes. Figure 2B shows the real and imaginary part (Z'' vs. Z') of the EIS spectra represented as Nyquist plots for (a) c-MWCNTs/Fe_3O_4/CHIT/GCE, (b) c-MWCNTs/Co_3O_4/CHIT/GCE, (c) c-MWCNTs/CHIT/GCE, (d) Fe_3O_4/CHIT/GCE, (e) Co_3O_4/CHIT/GCE, (f) GCE, and (g) CHIT/GCE using 5.0 mM $Fe(CN)_6^{3-/4-}$ as the electrolyte.

The electron transfer resistance (R_{ct}) value for the 5.0 mM $Fe(CN)_6^{3-/4-}$ redox probe was evaluated as the diameter of the high-frequency semicircle in the Nyquist plots [38]. It can be seen from the figure that the R_{ct} value of bare GCE (1250 Ω) (curve b) remarkably increased when the electrode was modified with CHIT (1600 Ω) (curve a). This result reveals that the CHIT layer limited the diffusion of the redox probe to the electrode surface. The R_{ct} of 5 mM $[Fe(CN)_6]^{3-/4-}$ at the Co_3O_4/CHIT/GCE (240 Ω) (curve c), Fe_3O_4/CHIT/GCE (200 Ω) (curve d) and c-MWCNTs/CHIT/GCE (65 Ω) (curve e) is much smaller than that at bare GCE (curve b) and CHIT/GCE (curve a).This result shows that MONPs and c-MWCNTs significantly increased the electron transfer properties of the modified electrode. For the c-MWCNTs/Co_3O_4/CHIT/GCE (25 Ω) (curve f), almost a straight line with a very low R_{ct} was observed indicating that the c-MWCNTs/Co_3O_4/CHIT composite had high electrical conductivity and thereby improved electron transfer. The smallest R_{ct} was observed with c-MWCNTs/Fe_3O_4/CHIT/GCE (20 Ω) (curve g) which attributed to synergistic action of the MONPs and c-MWCNTs that promoted electron transfer.

CV was performed in order to investigate the electrochemical behaviour of TCNQ at c-MWCNTs/Fe_3O_4/TCNQ/CHIT/GCE and the corresponding voltammogram in 0.05 M PBS (pH 7.0) is shown in Figure 3. The CV exhibit two anodic peaks ($E_{pa1=}$+0.25 and E_{pa2}=-0.05 V) at forward scan of potential and two cathodic peaks ($E_{pc1=}$+0.10 and E_{pc2}=-0.10 V) in backward scan of the potential. The observed CVs were quite similar to those reported earlier for different electrodes. Quite similar voltammograms for TCNQ were observed at different electrode surfaces [39] The differences in peak shape and position may be attributed to the surface modifications. The anodic peaks and cathodic peaks correspond to the following electrochemical processes: $TCNQ \rightleftharpoons TCNQ^-$ and $TCNQ^- \rightleftharpoons TCNQ^{2-}$

c-MWCNTs/Fe_3O_4/TCNQ/CHIT/GCE provided a stable electrochemical response during continous potential cycling between -1.0–1.0 V in 0.05 M PBS at 50 mVs^{-1} (data not shown), indicated that the CHIT matrix could prevent mediator from leakage efficiently. Figure 3 (inset) depicts the CVs of c-MWCNTs/Fe_3O_4/TCNQ/CHIT/GCE obtained at different scan rates ranging from 10 to 100 mVs^{-1}. This figure clearly shows that the peak currents increased with the increasing scan rate, while peak potential separation was nearly independent of the scan rates which indicated that the electron transfer of TCNQ on the surface of the electrode was quite reversible. Furthermore, the ratio of the oxidation peak current to reduction peak current (i_{pa}/i_{pc}) is close to unity which is the other evidence to demostrate the reversibility [40, 41]. CVs of the c-MWCNTs/Fe_3O_4/TCNQ/CHIT/GCE at different scan rates show that both anodic and cathodic peak currents are proportional to the square root of scan rate ($v^{1/2}$) for the scan rates changed from 10 to 100 mVs^{-1}. Figure 3 (inset) showed a linear increase in peak current with square root of potential scan rate ($v^{1/2}$) with a slope of 7.17 $mV^{1/2}\ s^{-1/2}\ \mu A^{-1}$ for the oxidation peak and a slope of −7.02 $mV^{1/2}\ s^{-1/2}\ \mu A^{-1}$ for the reduction peak. These results reveal that the redox behaviour of the c-MWCNTs/Fe_3O_4/TCNQ/CHIT/GCE is controlled by diffusion where electron transferred to and from the redox centers of the TCNQ involved diffusion. Similar results with different mediator based electrodes were also reported [42, 43].

Fig. 3. Cyclic voltammogram of c-MWCNTs/Fe_3O_4/TCNQ/CHIT/GCE (inset) CVs of c-MWCNTs/Fe_3O_4/TCNQ/CHIT/GCE in 0.05 M PBS containing 0.1 M KCl at 10, 25, 50, 75, 100 mVs^{-1} (from internal to external). (inset) plots of peak currents vs. square root of scan rate.

3.3. Optimization of electrode composition and working conditions

To determine the optimum composition of the composite, effects of c-MWCNTs, MONPs and TCNQ concentration and enzyme loading were investigated. Moreover, the experimental parameters affecting the sensitivity of the biosensors were optimized in terms of pH and

applied potential. All optimization studies were performed in 0.05 M PBS (pH 7.0) containing 0.1 mM xanthine and response currents of the biosensor were measured.

Different c-MWCNT concentrations (0.5 mg mL^{-1}; 1.0 mg mL^{-1}; 1.5 mg mL^{-1}; 2.0 mg mL^{-1}; 2.5 mg mL^{-1}) were tested to detect the optimum c-MWCNT amount. The highest current response was obtained by using 1.0 mg mL^{-1} c-MWCNT. Higher c-MWCNT concentrations did not improve the biosensor response. This optimum concentration (1 mg mL^{-1}) was used in the construction of all XOD/c-MWCNTs/MONPs/TCNQ/CHIT/GCEs. A study was carried out to investigate the effect of metal oxide nanoparticle amount on the biosensor response. Fe_3O_4 or Co_3O_4 amount was varied as 0.25 mg mL^{-1}; 0.5 mg mL^{-1}; 1.0 mg mL^{-1}; 2.0 mg mL^{-1} and 3.0 mg mL^{-1} while the c-MWCNT, TCNQ and enzyme amounts kept constant. The experiment was performed by injecting 0.1 mM xanthine into 0.05 M PBS (pH 7.0). The highest biosensor response was obtained with 1.0 mg mL^{-1} Fe_3O_4 and 0.5 mg mL^{-1} Co_3O_4 and these amounts were used for all further experiments.The amount of TCNQ, which plays the role of electron transfer mediator has a strong effect on response current [44]. Therefore, the amount of TCNQ used was optimized for both biosensors. TCNQ amount was varied between 1 mg mL^{-1} and 12 mg mL^{-1}. The response of the XOD/c-MWCNTs/Fe_3O_4/TCNQ/CHIT/GCE increased with the mediator amount up to 6 mg mL^{-1} and then the biosensor response decreased with increasing TCNQ amount. For the XOD/c-MWCNTs/Co_3O_4/TCNQ/CHIT/GCE the highest response was achieved with 9 mg mL^{-1} TCNQ.

The effect of enzyme loading into c-MWCNTs/MONPs/TCNQ/CHIT/GCE composite was examined in order to enhance the sensitivity of the xanthine biosensors. Various amounts of XOD within the biosensor matrix were investigated, namely, 0.062; 0.12; 0.25; 0.33 and 0.50 U. The amperometric responses of the c-MWCNTs/MONPs/TCNQ/CHIT/GCEs in 0.05 M PBS containing 0.1 mM xanthine were measured. The xanthine responses of various compositions of XOD on the c-MWCNTs/MONPs/TCNQ/CHIT composite modified electrodes are shown in Figure 4A. The biosensor response increased by raising the loading of XOD from 0.062 to 0.25 U and then decreased with enzyme loading of 0.33 and 0.50 units of

XOD with both biosensors. This decrease in response current is due to the thickness of the enzyme layer blocking diffusion of xanthine to the electrode surface. Thus, 0.25 units of XOD was used for all further experiments.

The operating potential is one of the most important parameters for biosensor response and selectivity. The response of XOD/c-MWCNTs/Co_3O_4/TCNQ/CHIT/GCE and XOD/c-MWCNTs/Fe_3O_4/TCNQ/CHIT/GCE to 0.1 mM xanthine was measured at different working potentials between (+0.15)–(+0.40) V. The highest biosensor response was obtained at +0.30 V. Thus, all further studies were carried out at +0.30 V.

In this study, in order to minmize the effects of potentially interfering substances exist in real samples, TCNQ, which is electrochemically oxidized at a lower potential, was selected as a mediator. The principle of operation of the xanthine biosensors follows the typical mechanism of the second generation amperometric biosensors and can be schematized as follows:

$$\text{Xanthine} + H_2O \xrightarrow{XOD_{ox}} \text{Uric}^{-}\text{acid}$$

$$XOD_{(red)} + TCNQ_{(ox)} \rightarrow XOD_{(ox)} + TCNQ_{(red)}$$

$$TCNQ_{(red)} \xrightarrow{\text{Electrode}(+0.30\,V} TCNQ_{(ox}$$

In the response mechanism of the biosensor $TCNQ_{(ox)}$ accepts electrons from the reduced xanthine oxidase and $TCNQ_{(red)}$ is produced. Then $TCNQ_{(red)}$ is reoxidized on the surface of the electrode at +0.30 V. The resulting current is directly proportional to xanthine concentration.

The pH of the medium is an other critical parameter for the sensitivity of the biosensors, because the activity of enzymes are pH dependent [45]. The effect of pH of PBS on the current response of the biosensors was studied over the pH range 6.0–8.0 in 0.05 M PBS at an interval of 0.5 pH unit. Fig. 4B depicts the amperometric responses of XOD/c-MWCNTs/Co_3O_4/TCNQ/CHIT/GCE and XOD/c-MWCNTs/Fe_3O_4/TCNQ/CHIT/GCE at different pH values with the presence of the 0.1 mM xanthine. The response of the biosensors increased with the increase of pH from 6.0 to 7.0 and reached a maximum response at pH 7.0 and then decreased. Thus, the optimum pH for the detection of xanthine was considered to be pH 7.0, and used in further studies. The optimal pH value of the free XOD was reported as pH 7–7.5, it can be concluded that the immobilization procedure used in this study and c-MWCNTs/MONPs/TCNQ/CHIT composite almost did not affect the optimum pH of XOD.

Fig. 4. Effect of (A) enzyme amount (B) pH on the response of the biosensors (a) XOD/c-MWCNTs/Fe_3O_4/TCNQ/CHIT/GCE (b) XOD/c-MWCNTs/Co_3O_4/TCNQ/CHIT/GCE (in 0.05 M PBS at +0.30 V, error bars show the standard deviation of three measurements)

3.4. Analytical characteristics of the biosensors

Figure 5 depicts the calibration curves and amperometric responses at (a) XOD/c-MWCNTs/Co_3O_4/TCNQ/CHIT/GCE and (b) XOD/c-MWCNTs/Fe_3O_4/TCNQ/CHIT/GCE for the addition of varying amounts of xanthine in a 0.05 M pH 7.0 PBS. The calibration curve for XOD/c-MWCNTs/Co_3O_4/TCNQ/CHIT/GCE shows a linear response to the concentration of xanthine in the range of 1.9×10^{-6}–1.2×10^{-4} M (R^2=0.9887). The detection limit was estimated to be 3.6×10^{-7} M when the signal-to-noise ratio is 3 and the sensitiviy of the biosensor was calculated to be 13.24 μA/mMcm^2. On the other hand, the linear response range of the XOD/c-MWCNTs/Fe_3O_4/TCNQ/CHIT/GCE for xanthine was 1.9×10^{-6}–2.3×10^{-4} M (R^2=0.9887). The linear working ranges of the presented biosensors are wider than most of the xanthine biosensors [19, 33, 35, 41, 46, 47]. The sensitiviy of the XOD/c-MWCNTs/Fe_3O_4/TCNQ/CHIT/GCE was calculated to be 25.07 μA/mMcm^2 which was about 1.9 fold higher than that of XOD/c-MWCNTs/Co_3O_4/TCNQ/CHIT/GCE. The detection limit

of the Fe_3O_4 based biosensor was 2.0×10^{-7} M (*S/N*=3), lower than that of Co_3O_4 based biosensor. These detection limits are much lower than the detection limits obtained in previously reported xanthine biosensors [33, 48-52] and is comparable to the value obtained in the PB modified screen printed electrode [34]. Both biosensors responded rapidly to changes in xanthine concentration, reaching 95% of the steady-state currents in less than 10 s which can be attributed to the existence of TCNQ as mediator of electron transfer and the high conductivity of the c-MWNTs and MONPs.

The apparent Michaelis–Menten constant (K_M^{app}), a reflection of the enzymatic affinity, is calculated to be 0.60 mM for XOD/c-MWCNTs/Co_3O_4/TCNQ/CHIT/GCE and 0.20 mM for XOD/c-MWCNTs/Fe_3O_4/TCNQ/CHIT/GCE according to the Lineweaver–Burk equation [53]. The K_M^{app} value of Fe_3O_4 based biosensor is lower than that of Co_3O_4 based biosensor suggesting a higher affinity towards xanthine and a good bioactivity. These values are lower than those reported with polypyrrole modified platinum electrode [33], polyvinylferrocenium modified platinium electrode [51], cobalt phthalocyanine modified carbon paste electrode [35] but higher than those reported with Fe_3O_4@APTES modified carbon paste electrode [52] and Ag-NPs/cysteine modified Au electrode [21] (Table 2).

Fig. 5. Calibration graphs and amperometric responses of (A) XOD/c-MWCNTs/Fe_3O_4/TCNQ/CHIT/GCE and (B) XOD/c-MWCNTs/Co_3O_4/TCNQ/CHIT/GCE in a stirred 0.05 M PBS (pH 7.0) after successive xanthine additions at +0.30 V.

To evaluate the repeatability of the xanthine biosensors successive calibration curves (n=5) were plotted by the use of the same biosensor. The relative standard deviation of the sensitivity values were found to be 3.0% for XOD/c-MWCNTs/Co_3O_4/TCNQ/CHIT/GCE and 3.5% for XOD/c-MWCNTs/Fe_3O_4/TCNQ/CHIT/GCE. These results demonstrated the good repeatability of the biosensors. Although, the Co_3O_4 based biosensor offered a better repeatability, no significant differences were observed for the purposed biosensors. The long term stability was studied by periodical measurements of the biosensor responses to 0.1 mM

xanthine in 0.05 M PBS (pH 7.0) at +0.30 V. The biosensors were stored at 4 °C in 0.05 M pH 7.0 PBS between the measurements. It was found that the current response at XOD/c-MWCNTs/Fe_3O_4/TCNQ/CHIT/GCE decreased about 15% in 15 days, and 30% in 30 days. The loss of the response current may be attributed to the xanthine oxidase enzymes which partly lose their bioactivity during storage. The response current at the XOD/c-MWCNTs/Co_3O_4/TCNQ/CHIT/GCE decreased to about 30% of its initial response current after 15 days. This indicates that XOD/c-MWCNTs/Fe_3O_4/TCNQ/CHIT/GCE showed a better long term stability.

The effect of common interfering species on the XOD/c-MWCNTs/Co_3O_4/TCNQ/CHIT/GCE and XOD/c-MWCNTs/Fe_3O_4/TCNQ/CHIT/GCE response was investigated. The interference experiment was carried out by the successive injection of xanthine (5.0×10^{-6} M) and interfering species (2.0×10^{-6} M) in 0.05 M PBS. When a stable baseline current was reached, xanthine was added and response was measured. Then the interfering substances was added and after that amperometric response was measured again. The biosensor response obtained for xanthine was accepted as 100% and compared with the biosensor responses obtained for the other possible interfering substances. Table 1 shows the results of the selectivity study. Compared to xanthine response, the interfering species yielded current response ranging from -1.0% (glucose) to 6.0% (ascorbic acid) at +0.30 V with both biosensors. These small responses for glucose, uric acid, ascorbic acid and sodium benzoate can be neglected. It can be concluded that, the presented xanthine biosensors shows high selectivity towards xanthine detection and this result can mainly be ascribed to the low operating potential of +0.30 V and presence of Nafion layer that can efficiently avoid interference. Moreover, no significant differences in selectivity were found for both biosensors.

Table 1. Results of interference experiments on the current response of 0.1 mM xanthine on (a) c-MWCNTs/Fe_3O_4/TCNQ/CHIT/GCE and (b) c-MWCNTs/Co_3O_4/TCNQ/CHIT/GCE

Interference substances	**Concentration[a] (mM)**	**Interference(%) (a)**	**Interference(%) (b)**
Glucose	0.002	-1	-1

Uric acid	0.002	4	3
Ascorbic acid	0.002	6	2
Sodium benzoat	0.002	-2	-2
Xanthine	0.005		

[a] Concentrations of interference substances in aqueous media.

To evaluate the performance of the developed xanthine biosensors, a comparison of different parameters obtained by various biosensors for xanthine detection was summarized in Table 2. It can be found that the XOD/c-MWCNTs/Fe_3O_4/TCNQ/CHIT/GCE and XOD/c-MWCNTs/Fe_3O_4/TCNQ/CHIT/GCE exhibited wider linear working ranges, lower detection limits and better sensitivities than most of the previous xanthine biosensors [33, 35, 46, 47, 54] The favorable analytical performance of the biosensors can be ascribed to the following aspects: (i) covalent immobilization of enzyme into c-MWCNTs/Co_3O_4/TCNQ/CHIT composite is likely to minimize the problem of enzyme leakage and thus increase its long-term stability, (ii) chitosan provides a biocompatible microenvironment around XOD to maintain its enzymatic activity, (iii) c-MWNTs and MONPs provided a conduction pathway to accelerate electron transfer due to their high conductivity, (iv) relatively low working potential of TCNQ minimizes the oxidation of electrochemically active compounds.

Table 2. Characteristics of various amperometric xanthine biosensors reported in recent years

Enzyme /Working potential	Electrode composition/Immobilization technique	Linearity/Detection limit	K_m mM	Response time	Storage stability	Reference
XO/+0.30 V vs. Ag/AgCl	Au/poly(mercapto-p-benzoquinone/GCE/Electropolymerization	1×10^{-6}–8×10^{-5} M	0.08	−	8 days (30% loss)	[46]
XO/+0.35 V vs. Ag/AgCl	Cobalt phthalocyanine/carbon+mineral oil/CPE	1×10^{-3}–1.5×10^{-2} M	−	−	60 days (60% loss)	[35]

XO/+0.7 V vs.Ag/AgCl	$CuPtCl_6$/GCE/Covalent immobilization	6×10^{-7}–2×10^{-4} M/0.10 µM	1.11	<15 s	7 days (30% loss)	[45]
XO/+0.1 V vs.Ag/AgCl	PB/PPy/Au- colloid/Au electrode/Adsorption	1.0×10^{-6}–2.0×10^{-5} M	0.04	–	–	[47]
XO/+0.7 V vs. SCE	Platinium-PPy/Ferrocenium/Pt electrode/Cross-linking	1×10^{-5}–4×10^{-4} M/1 µM	1.33	4 min.	45 days	[33]
XO/0.05 V vs. Ag/AgCl	PB/SPTE/Cross-linking	1×10^{-7}–4.98×10^{-6} M /0.10 µM	0.004	–	–	[34]
XO/+0.4 V vs. Ag/AgCl	Au-NPs/PVF/Pt	2.5×10^{-6}–$5.6\ 10^{-4}$ M/0.75 µM	0.393	–	18 days (40% loss)	[49]
	Pt-NPs/PVF/Pt/Electro deposition	2.0×10^{-6}–$6.6\ 10^{-4}$ M /0.60 µM	0.286		23 days (40% loss)	
XO/+0.5 V vs. Ag/AgCl	PVF-perchlorate matrix/Pt electrode/Electro deposition	4.3×10^{-7}–2.84×10^{-3} M/0.13 µM	3.454	15 s	25 days (42% loss)	[54]
XO/+0.05 V vs. Ag/AgCl	Phenazine methosulfate as mediator/ Edge-plane pyrolytic graphite/ Adsorpsion	1.0×10^{-5}–1.8×10^{-3} M/0.25 nM	1.0 ± 0.1	–	4 weeks (22% loss)	[55]
XO/+0.25 V vs. Ag/AgCl	1,4-benzoquinone/CPE	1.9×10^{-7} -5.5×10^{-6} M and 5.2×10^{-5}–8.2×10^{-4} M/0.1 µM	–	100 s	14 days	[19]
XO/+0.30 V vs. Ag/AgCl	PVF/CPE/Cross-linking	1.9×10^{-7}–2.1×10^{-6} M; 1.9×10^{-6} -1.0×10^{-5} M and 5.2×10^{-5}		50 s	7 days	

		-8.2×10^{-4} M/0.1 µM				
XO/+0.50 V vs. Ag/AgCl	CHIT/Fe-NPs@Au/PGE/Electro deposition	$1\times10^{-7}-3\times10^{-4}$ M/0.1 µM	−	3s	100 days (25% loss)	[21]
XO/+0.35 V vs. Ag/AgCl	Poly(glycidyl methacrylate-co-vinylferrocene)/MWCNT/PGE/Covalent immobilization	$2\times10^{-6}-2.8\times10^{-5}$ M; $2.8\times10^{-5}-4.6\times10^{-5}$; $4.6\times10^{-5}-8.6\times10^{-5}$/0.12 µM	−	4 s	25 days (30% loss)	[41]
XO/+0.30 V vs. Ag/AgCl	c-MWCNTs/Fe_3O_4/TCNQ/CHIT/GCE	$1.9\times10^{-6}-2.3\times10^{-4}$ M/0.20 µM	0.20	‹10 s	30 days (30% loss)	This work
	c-MWCNTs/Co_3O_4/TCNQ/CHIT/GCE	$1.9\times10^{-6}-1.2\times10^{-4}$ M/0.36 µM	0.60			
	Covalent immobilization				15 days (30% loss)	

CPE: Carbon paste electrode; PB: Prussian blue; SPTE:Screen printed electrode; PGE: Pencil graphite electrode; PPy: Polypyrrole; PVF: Polyvinylferrocenium

3.5. Analysis of coffee sample

The practical application of the developed biosensors was evaluated by means of the xanthine analysis in coffee sample. Roasted coffee sample was supplied from a local market. The coffee sample (1.0 g) was boiled in 100 mL of 0.1 M NaOH for 30 min and filtered through a Whatman 41 filter paper. The filtrate was cooled to room temperature and diluted to 150 mL. Xanthine level in coffee sample was determined by standard addition method. For this purpose, additions of standard xanthine solution were made to several portions of the coffee extract, and a multiple addition calibration curve was obtained. The xanthine concentration in coffee sample was found to be 1.44±0.09 mg L^{-1} (n=3) with XOD/c-MWCNTs/Fe_3O_4/TCNQ/CHIT/GCE and 1.49±0.05 mg L^{-1} (n=3) with XOD/c-

MWCNTs/Co_3O_4/TCNQ/CHIT/GCE. The recovery studies were performed to provide further support for the applicability of the method (Table 3). The mean recoveries ranged between 99 and 103 %. These results indicated that the biosensors suffered from little interference from sample matrix and thus can be used to determine xanthine in coffee samples.

The results were also compared with those obtained by the HPLC method. A comparison of two methods for xanthine determination in coffee sample is presented in Table 4. The accuracy of the presented method was also checked by t-test. The *t* value is 1.53 for XOD/c-MWCNTs/Fe_3O_4/TCNQ/CHIT/GCE and 0.41 for XOD/c-MWCNTs/Co_3O_4/TCNQ/CHIT/GCE at 95% confidence level, for which t_{critic} is 2.78. It shows that there is no significant difference between the results obtained for the coffee sample by the proposed biosensors and those obtained by the HPLC method. It can be concluded that the xanthine biosensors could be applied in real samples satisfactorily and efficiently.

Table 3. The result of the recovery studies of standard additions to coffee samples obtained with two xanthine biosensors.

XOD/c-MWCNTs/Fe_3O_4/TCNQ/CHIT/GCE*			**XOD/c-MWCNTs/Co_3O_4/TCNQ/CHIT/GCE**		
Xanthine added (mg L^{-1})	Xanthine found (mg L^{-1})	Recovery %	Xanthine added (mg L^{-1})**	Xanthine found (mg L^{-1})	Recovery %
–	1.44±0.09	–	–	1.49±0.05	–
1.48	2.89±0.07	101.5±8.1	1.48	2.96±0.06	99.5±7.9
4.35	5.82±0.14	101.3±3.9	4.35	5.87±0.19	100.5±4.2
7.11	8.82±0.60	103.4±7.1	7.11	8.71±0.75	103.0±6.9

*Results are expressed as $\bar{x} \pm ts/\sqrt{N}$ (*n*= 3).

Table 4. Comparison between the results obtained by the proposed biosensors and by HPLC method for the determination of xanthine in coffee sample

Experiment No	HPLC	XOD/c-MWCNTs/Fe_3O_4/TCNQ/CHIT/GCE*	XOD/c-MWCNTs/Co_3O_4/TCNQ/CHIT/GCE
1	1.48	1.50	1.40
2	1.46	1.48	1.46
3	1.50	1.47	1.47
	1.47±0.04	1.49±0.05	1.44±0.09

*Results are expressed as $\bar{x} \pm ts/\sqrt{N}$ (n= 3).

4. Conclusions

Two xanthine biosensors were successfully developed using c-MWCNTs, MONPs, TCNQ and CHIT composites. In these composites c-MWNTs and MONPs act as efficient pathways for electron transfer, CHIT is an biocompatible polymeric binder as backbone, and TCNQ is an electron transfer mediator that minimizes the effect of interferences by lowering the operating potential. From the comparison of the analytical characteristics of the purposed biosensors, it can be concluded that both of them can be used for the determination of xanthine. However, XOD/c-MWCNTs/Fe_3O_4/TCNQ/CHIT/GCE showed a rather good long term stability, higher sensitivity, lower detection limit and wider linear working range. Furthermore, the developed biosensors have favorable analytical performance than most of the other xanthine biosensors reported in the literature and the proposed method is a good alternative to previously described methods because of its high selectivity and good sensitivity.

Acknowledgments

The authors gratefully acknowledge Prof. Dr. Abdülkadir AKAY and Res. Asst. E. Kübra INAL (Ankara University, Department of Chemistry) for HPLC analysis.

Conflict of interest

The authors declare no competing financial interest.

References

[1] N.J. Ronkainen, H.B. Halsall, W.R. Heineman, Electrochemical biosensors, Chem. Soc. Rev. 39(5) (2010) 1747-1763.

[2] P.E. Erden, E. Kilic, A review of enzymatic uric acid biosensors based on amperometric detection, Talanta 107 (2013) 312–323.

[3] C.B. Jacobs, M.J. Peairs, B.J. Venton, Review:Carbon nanotube based electrochemical sensors for biomolecules, Anal. Chim. Acta 662(2) (2010) 105-127.

[4] W. Yang, K.R. Ratinac, S.P. Ringer, P. Thordarson, J.J. Gooding, F. Braet, Carbon nanomaterials in biosensors: should you use nanotubes or graphene?, Angew. Chem. Int. Ed. 49(12) (2010) 2114-2138.

[5] X. Shi, W. Gu, B. Li, N. Chen, K. Zhao, Y. Xian, Enzymatic biosensors based on the use of metal oxide nanoparticles, Microchim. Acta 181(1-2) (2014) 1-22.

[6] P.R. Solanki, A. Kaushik, V.V. Agrawal, B.D. Malhotra, Nanostructured metal oxide-based biosensors, NPG Asia Mater. 3(1) (2011) 17-24.

[7] R. Devi, C.S. Pundir, Construction and application of an amperometric uric acid biosensor based on covalent immobilization of uricase on iron oxide nanoparticles/chitosan-g-polyaniline composite film electrodeposited on Pt electrode, Sensor. Actuat. B-Chem. 193 (2014) 608-615.

[8] B.Dalkiran, C. Kaçar, P.E. Erden, E. Kilic, Amperometric xanthine biosensors based on chitosan-Co_3O_4-multiwall carbon nanotube modified glassy carbon electrode, Sensor. Actuat. B-Chem. 200 (2014) 83-91.

[9] C. Karuppiah, S. Palanisamy, S.M. Chen, V. Veeramani, P. Periakaruppan, A novel enzymatic glucose biosensor and sensitive non-enzymatic hydrogen peroxide sensor based on graphene and cobalt oxide nanoparticles composite modified glassy carbon electrode, Sensor. Actuat. B-Chem.196 (2014) 450-456.

[10] M. Shamsipur, M. Najafi, M.R.M. Hosseini, Highly improved electrooxidation of glucose at a nickel (II) oxide/multi-walled carbon nanotube modified glassy carbon electrode, Bioelectrochem.77(2) (2010) 120-124.

[11] A.P. Periasamy, S. Yang, S.M. Chen, Preparation and characterization of bismuth oxide nanoparticles-multiwalled carbon nanotube composite for the development of horseradish peroxidase based H_2O_2 biosensor, Talanta 87 (2011) 15-23.

[12] T.T. Baby, S. Ramaprabhu, SiO_2 coated Fe_3O_4 magnetic nanoparticle dispersed multiwalled carbon nanotubes based amperometric glucose biosensor, Talanta 80(5) (2010) 2016-2022.

[13] H.J. Chen, Z.H. Zhang, L.J. Luo, S.Z. Yao, Surface-imprinted chitosan-coated magnetic nanoparticles modified multi-walled carbon nanotubes biosensor for detection of bovine serum albümin, Sensor. Actuat. B-Chem. 163(1) (2012) 76-83.

[14] S. Palanisamy, S. Cheemalapati, S.M. Chen, Highly sensitive and selective hydrogen peroxide biosensor based on hemoglobin immobilized at multiwalled carbon nanotubes–zinc oxide composite electrode, Anal. Biochem. 429(2) (2012) 108-115.

[15] J. Li, D. Kuang, Y. Feng, F. Zhang, M. Liu, Glucose biosensor based on glucose oxidase immobilized on a nanofilm composed of mesoporous hydroxyapatite, titanium dioxide, and modified with multi-walled carbon nanotubes, Microchim. Acta 176(1-2) (2012) 73-80.

[16] S. Lata, B. Batra, N. Karwasra, C.S. Pundir, An amperometric H_2O_2 biosensor based on cytochrome c immobilized onto nickel oxide nanoparticles/carboxylated multiwalled carbon nanotubes/polyaniline modified gold electrode, Process Biochem. 47(6) (2012) 992-998.

[17] B. Batra, S. Lata, C.S. Pundir, Construction of an improved amperometric acrylamide biosensor based on hemoglobin immobilized onto carboxylated multi-walled carbon nanotubes/iron oxide nanoparticles/chitosan composite film, Bioproc. Biosyst. Eng. 36(11) (2013) 1591-1599.

[18] C.S. Pundir, R. Devi, Biosensing methods for xanthine determination: A review, Enzyme Microb. Tech. 57 (2014) 55-62.

[19] P.E. Erden, Ş. Pekyardımcı, E. Kılıç, Amperometric enzyme electrodes for xanthine determination with different mediators, Acta Chim. Slov. 59 (2012) 824-832.

[20] S. Gunasekaran, G. Sankari, S. Ponnusamy, Vibrational spectral investigation on xanthine and its derivatives theophylline, caffeine and theobromine, Spectrochim. Acta A Mol. Biomol. Spectrosc. 61(1) (2005)117-127.

[21] R. Devi, B. Batra, S. Lata, S. Yadav, C.H. Pundir, A method for determination of xanthine in meat by amperometric biosensor based on silver nanoparticles/cysteine modified Au electrode, Process Biochem. 48 (2013) 242–249.

[22] R.S. Pagliarussi, L.A. Freitas, J.K. Bastos, A quantitative method for the analysis of xanthine alkaloids in Paullinia cupana (guarana) by capillary column gas chromatography, J. Sep. Sci. 25(5-6) (2002) 371-374.

[23] G.F. Mu, F. Luan, L.N. Xu, F.L. Hu, H.T. Liu, Y. Gao, Determination of purines in soybean milk by capillary electrophoresis in comparison with high performance liquid chromatography, Anal. Methods 4(10) (2012) 3386-3391.

[24] R. Boulieu, C. Bory, P. Baltassat, C. Gonnet, High-performance liquid chromatographic determination of hypoxanthine and xanthine in biological fluids, J. Chroma. B: Bio. Sci. App. 233(1) (1982) 131-140.

[25] M. Czauderna, J. Kowalczyk, Simultaneous measurement of allantoin, uric acid, xanthine and hypoxanthine in blood by high-performance liquid chromatography, J. Chroma. B: Bio. Sci. App. 704(1) (1997) 89-98.

[26] J.R. Klinenberg, S. Goldfinger, K.H. Bradley, J.E. Seegmiller, An enzymatic spectrophotometric method for the determination of xanthine and hypoxanthine, Clinical Chem. 13(10) (1967) 834-846.

[27] M. Saadaoui, A. Sánchez, P. Díez, N. Raouafi, J.M. Pingarrón, R. Villalonga, Amperometric xanthine biosensors using glassy carbon electrodes modified with electrografted porous silica nanomaterials loaded with xanthine oxidase, Microchim. Acta 183(6) (2016) 2023-2030.

[28] S. Sadeghi, E. Fooladi, M. Malekaneh, A nanocomposite/crude extract enzyme-based xanthine biosensor, Anal. Biochem. 464 (2016) 51-59.

[29] K. Thandavan, S. Gandhi, S. Sethuraman, J.B.B. Rayappan, U.M. Krishnan, Development of electrochemical biosensor with nano-interface for xanthine sensing–A novel approach for fish freshness estimation, Food Chem. 139(1) (2013) 963-969.

[30] E. Gonzalez, F. Pariente, E. Lorenzo, L. Hernandez, Amperometric sensor for hypoxanthine and xanthine based on the detection of uric acid, Anal. Chim. Acta 242 (1991) 267-273.

[31] S. Hu, C. Xu, J. Luo, J. Luo, D. Cui, Biosensor for detection of hypoxanthine based on xanthine oxidase immobilized on chemically modified carbon paste electrode, Anal. Chim. Acta 412(1) (2000) 55-61.

[32] A. Chaubey, B.D. Malhotra, Mediated biosensors, Biosens. Bioelectron. 17(6) (2002) 441-456.

[33] F. Arslan, A. Yaşar, E. Kilic, An amperometric biosensor for xanthine determination prepared from xanthine oxidase immobilized in polypyrrole film, Artif. Cell. Blood Sub. 34(1) (2006) 113-128.

[34] Y. Teng, C. Chen, C. Zhou, H. Zhao, M. Lan, Disposable amperometric biosensors based on xanthine oxidase immobilized in the Prussian blue modified screen-printed three-electrode system, Sci. China Chem. 53(12) (2010) 2581-2586.

[35] E. Kilinc, A. Erdem, L. Gokgunnec, T. Dalbasti, M. Karaoglan, M. Ozsoz, Buttermilk based cobalt phthalocyanine dispersed ferricyanide mediated amperometric biosensor for the determination of xanthine, Electroanal. 10(4) (1998) 273-275.

[36] P.C. Pandey, D.S. Chauhan, V. Singh, Poly (indole-6-carboxylic acid) and tetracyanoquinodimethane-modified electrode for selective oxidation of dopamine, Electrochim. Acta 54(8) (2009) 2266-2270.

[37] J. Wang, Analytical electrochemistry, John Wiley & Sons 2006.

[38] E.P. Randviir, C.E. Banks, Electrochemical impedance spectroscopy: an overview of bioanalytical applications, Anal.Method. 5(5) (2013) 1098-1115.

[39] A.S.N. Murthy, A.R.L. Gupta, NADH sensor with electrochemically modified TCNQ electrode, Anal. Chim. Acta 289 (1994) 43-46.

[40] A. J. Bard, L. R. Faulkner, Electrochemical Methods:Fundamentals and Applications, Wiley, New York 1980,

[41] M. Dervisevic, E. Custiuc, E. Cevik, M. Senel, Construction of novel xanthine biosensor by using polymeric mediator/MWCNT nanocomposite layer for fish freshness detection, Food Chem. 181 (2015) 277-283.

[42] J.D. Qiu, J. Huang, R.P. Liang, Nanocomposite film based on graphene oxide for high performance flexible glucose biosensor, Sens. Actuat. B 160 (2011) 287–294.

[43] D. Shan, W. Yao, H. Xue, Electrochemical study of ferrocenemethanol-modified layered double hydroxides composite matrix: Application to glucose amperometric biosensor, Biosens.Bioelec. 23 (2007) 432–437.

[44] C.X. Liu, H.M. Liu, Q.D. Yang, Q. Tian, X.X. Cai, Development of amperometric lactate biosensor modified with Pt-black nanoparticles for rapid assay, Chin. J. Anal. Chem. 37(4) (2009) 624-628.

[45] J. Pei, X.Y. Li, Xanthine and hypoxanthine sensors based on xanthine oxidase immobilized on a $CuPtCl_6$ chemically modified electrode and liquid chromatography electrochemical detection, Anal. Chim. Acta 414 (2000) 205–213.

[46] G. Arai, S. Takahashi, I. Yasumori, Xanthine and hypoxanthine sensors based on xanthine oxidase immobilized in poly(mercapto-p-benzoquinone) film, J. Electroanal. Chem. 410 (1996) 173-179.

[47] Y. Liu, L. Nie, W. Tao, S. Yao, Amperometric study of Au-Colloid function on Xanthine biosensor based on xanthine oxidase immobilized in polypyrrole layer, Electroanal. 16 (2004) 1271−1278.

[48] T. Dodevska, E. Horozova, N. Dimeva, Design of an amperometric xanthine biosensor based on a graphite transducer patterned with noble metal microparticles. Cent. Eur. J. Chem. 8(1) (2010) 19–27.

[49] S.Z. Bas, H. Gulce, S. Yıldız, A. Gulce, Amperometric biosensors based on deposition of gold and platinum nanoparticles on polyvinylferrocene modified electrode for xanthine detection, Talanta 87 (2011) 189– 196.

[50] R. Devi, M. Thakur, C.S. Pundir, Construction and application of an amperometricxanthine biosensor based on zinc oxide nanoparticles–polypyrrole compositefilm, Biosens. Bioelectron. 26 (2011) 3420-3426.

[51] R. Devi, S. Yadav, C.S. Pundir, Au-colloids-polypyrrole nanocomposite filmbased xanthine biosensor, Colloids Surf A Physicochem. Eng. Asp. 394 (2012) 38-45.

[52] P. Diez, R. Villalonga, M.L. Villalonga, J.M. Pingarron, Supramolecular immobilization of redox enzymes on cyclodextrin-coated magnetic nanoparticles for biosensing applications, J. Colloid Interface Sci. 386 (2012) 181-188.

[53] M.D. Fusco, C. Tortolini, D. Deriu, F. Mazzei, Laccase-based biosensor for the determination of polyphenol index in wine, Talanta 81 (2010) 235–240.

[54] S.Z.Bas, H. Gulce, S. Yıldız, Amperometric xanthine biosensors based on electrodeposition of platinum on polyvinylferrocenium coated Pt electrode. J. Mol. Catal. B: Enzym. 72 (2011) 282-288.

[55] P. Kalimuthu, S. Leimkuhler, P.V. Bernhardt, Low-potential amperometric enzyme biosensor for xanthine and hypoxanthine, Anal. Chem. 84 (2012) 10359−10365.

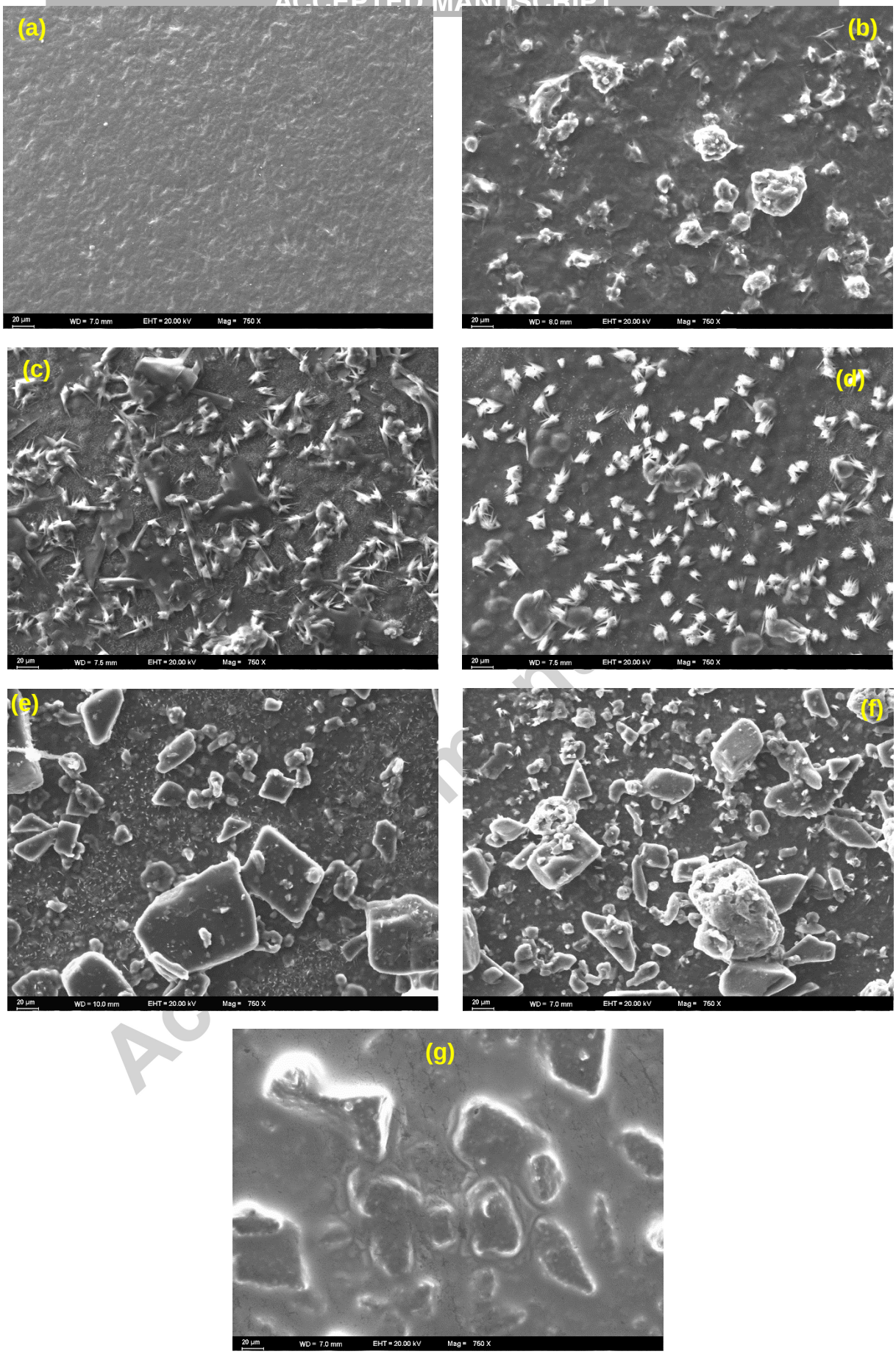

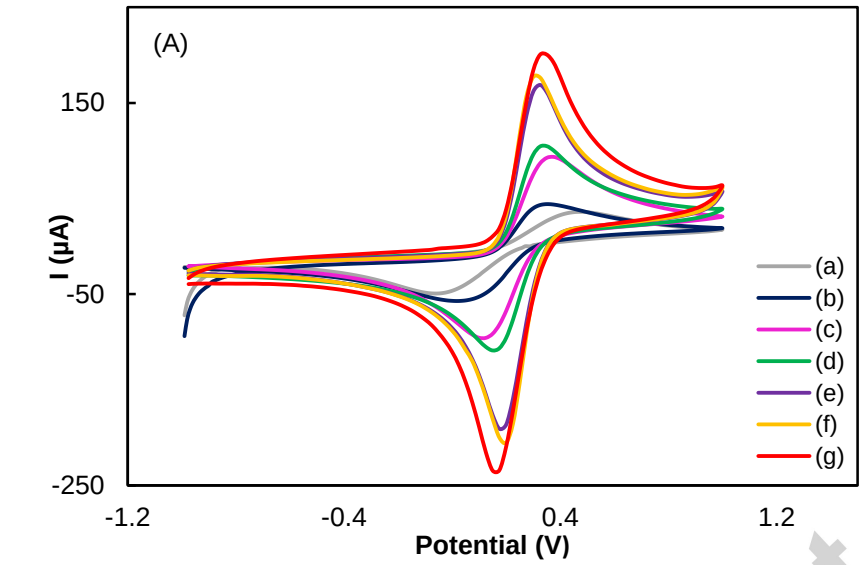

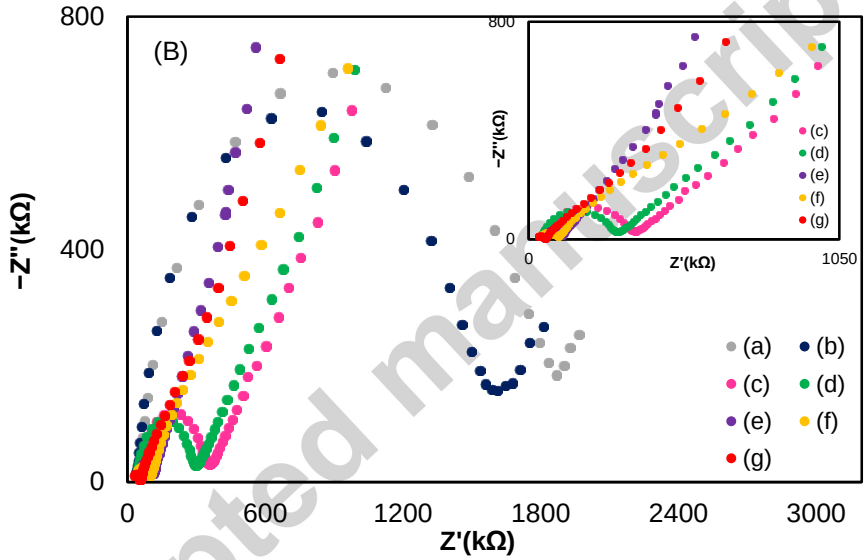

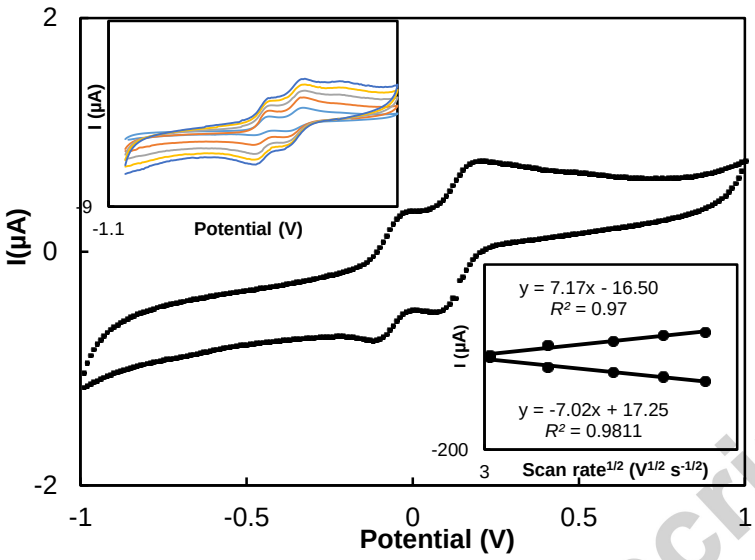

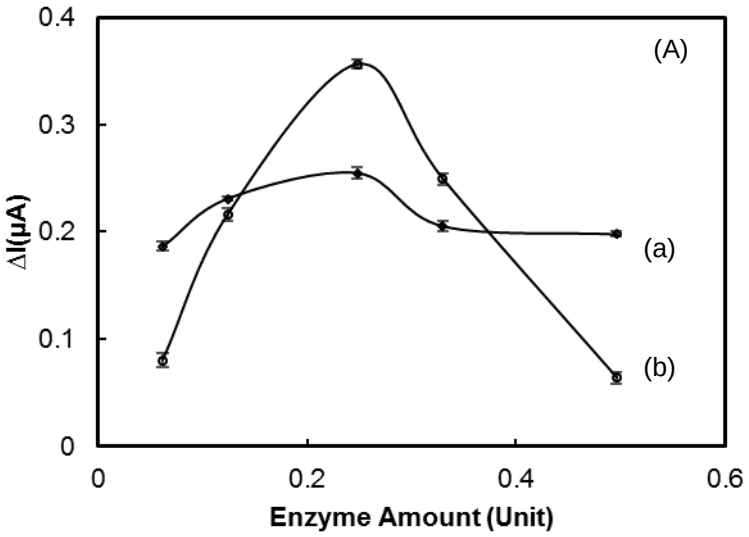

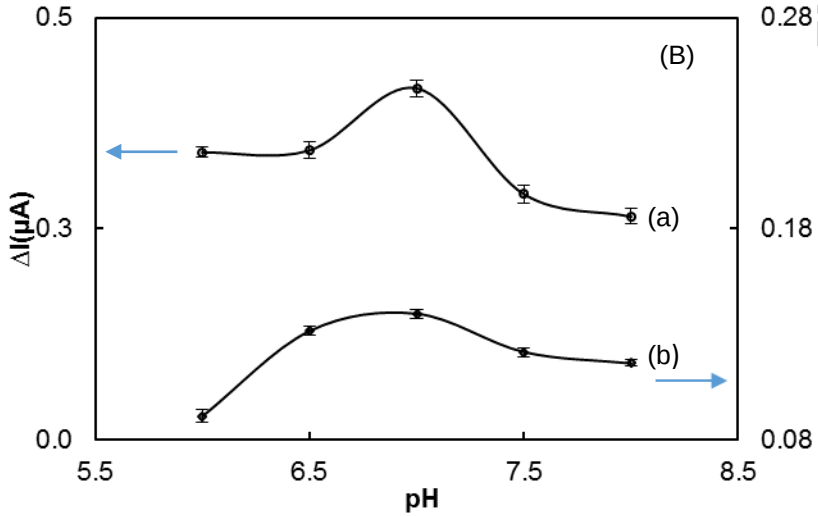

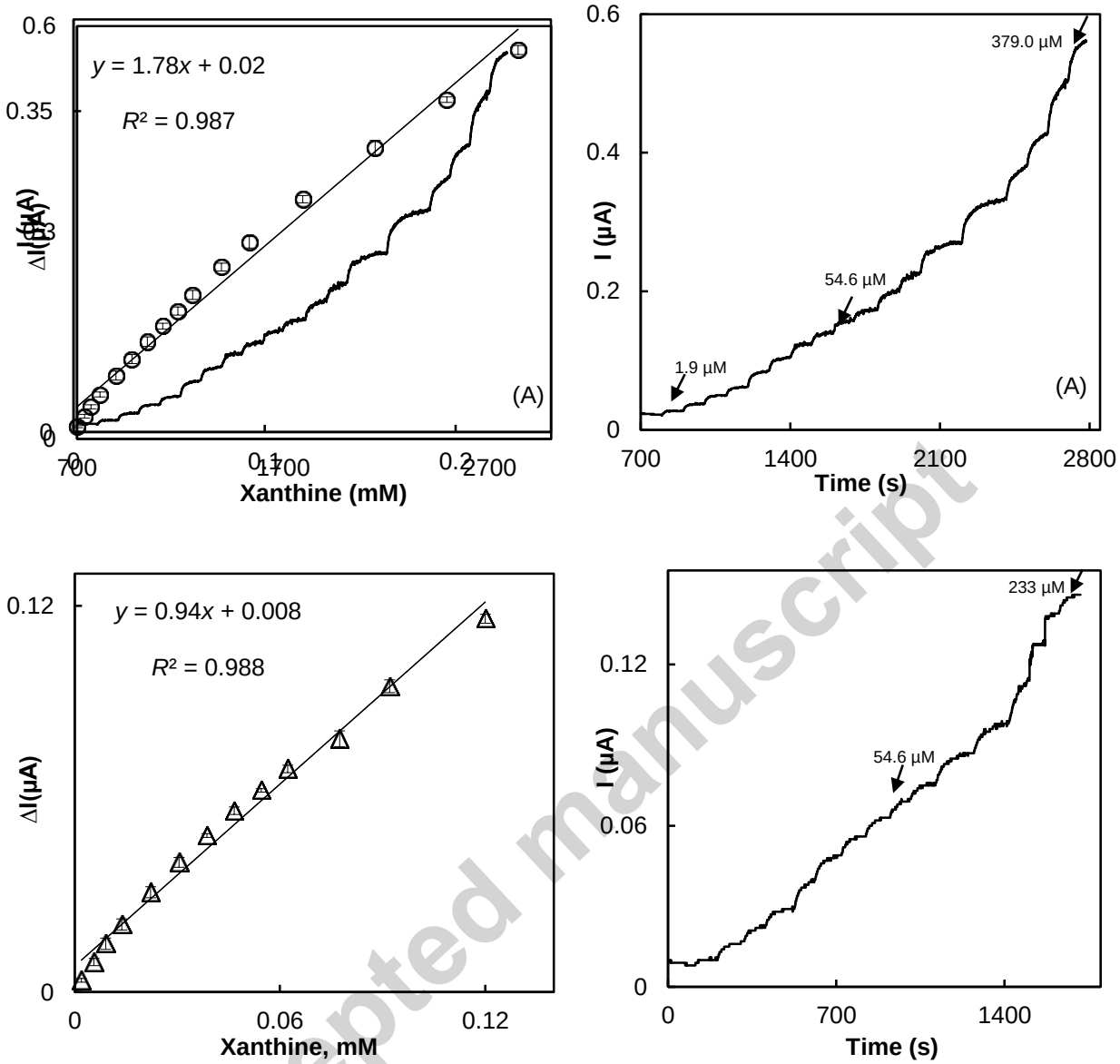

Highlights

- Xanthine biosensors based on Co_3O_4-MWCNT-TCNQ and Fe_3O_4-MWCNT-TCNQ were fabricated
- The analytical characteristics of the biosensors were compared
- The Fe_3O_4 based biosensor exhibited lower detection limit and higher sensitivity
- The presented biosensors were successfully applied to real sample analysis